ELSEVIER

Polymer 40 (1999) 3451–3462

polymer

Kinetic analysis of an asymmetrical DSC peak in the curing of an unsaturated polyester resin catalysed with MEKP and cobalt octoate

J.L. Martín*

Laboratori de Termodinàmica, E.T.S.E.I.Barcelona. Universitat Politècnica de Catalunya, Av. Diagonal, 647 08028 Barcelona, Spain

Received 26 September 1996; received in revised form 27 May 1998; accepted 14 July 1998

Abstract

In this paper, the curing of an unsaturated polyester resin catalysed with methyl ethyl ketone peroxide (MEKP) and cobalt octoate as the promoter, is studied at different heating rates. Given the non-symmetrical shape of differential scanning calorimetry (DSC) curves, it has been assumed that they would represent two independent reactions. The objective of this work has been to obtain a set of kinetic parameters for each DSC peak, which describe the overall cure process, using an empirical kinetic model of the form:

$$\frac{\mathrm{d}\alpha}{\mathrm{d}t}=yk_1f(\alpha_1)+(1-y)k_2f(\alpha_2)$$

where y is the fraction corresponding to the heat released during the first reaction, and k_i represents the rate constant for each process whose temperature dependence is an Arrhenius-type equation. With regard to $f(\alpha)$, two different kinetic functions have been employed: $(1-\alpha)^n$ and $\alpha^m(1-\alpha)^n$. The corresponding software to compute the degree of conversion α_1 and α_2, and the kinetic parameters, has been developed. The kinetic parameters obtained considering two independent reactions and an autocatalysed function $f(\alpha)$, fit better than the DSC experimental data $(\mathrm{d}\alpha/\mathrm{d}t,T)_{\mathrm{exp}}$, than those obtained when a single kinetic process is considered. The activation energies for each process are in accordance with tabulated values for typical free-radical polymerizations, induced by redox and thermal decomposition of the peroxides. © 1999 Elsevier Science Ltd. All rights reserved.

Keywords: Thermosetting; Curing; Kinetic analysis

1. Introduction

The unsaturated polyester (UP) resin is one of the most used thermosetting materials for composite applications [1], as the preparation of structural parts of automobiles, building materials, coating materials, electrical parts, etc. Since UP resin and thermosetting resins, in general, contain reactant groups, their processing requires an understanding of the reaction kinetics of polymerization during cure. The composition of the groups of reactant contained in the UP resin influences not only the curing rate, but also the final mechanical properties of the material. For instance, given the exothermicity of these materials, the control of temperature during the cure is of great importance for the quality of the product [2].

The differential scanning calorimetry (DSC) technique is commonly used for monitoring the process and for evaluating not only the heat of reaction, but also the reaction kinetics [3,4]. In this technique, it is common to assume that the rate of evolution of exchanged heat is strictly proportional to the rate of the global chemical reaction(s), at any instant, as follows [5,6]:

$$\frac{\mathrm{d}H}{\mathrm{d}t}=\Delta H_{\mathrm{R}}\frac{\mathrm{d}\alpha}{\mathrm{d}t}, \qquad (1)$$

where dH/dt is the heat generated by time unit or heat flow (DSC ordinate), dα/dt is the rate of reaction, and ΔH_{R} is the heat of reaction obtained as the area of the DSC thermogram. Therefore, it is possible to evaluate the reaction rate dα/dt at the time t, and the degree of conversion α reached at the time t, by means of the following expressions:

$$\frac{\mathrm{d}\alpha}{\mathrm{d}t}=\frac{1}{\Delta H_{\mathrm{R}}}\frac{\mathrm{d}H}{\mathrm{d}t},\quad \alpha=\frac{\Delta H_t}{\Delta H_{\mathrm{R}}}, \qquad (2)$$

where ΔH_t is the heat released up to the time t, and it can be obtained by integration of the calorimetric signal dH/dt up to time t.

In order to model the curing behaviour of a UP resin using DSC, theoretical methods [7–10] based on the concept of free-radical polymerization with its three steps: initiation,

---

* E-mail: jlmartin@mmt.upc.es

PII: S0032-3861(98)00556-4

propagation and termination, have been used successfully. These methods are of great interest in understanding the curing chemistry of UP resins, but their complexity is such that, for practical purposes, it is more convenient to use an empirical kinetic method [11–14]. In the present work, an empirical method will be used to obtain kinetic parameters of the curing of a UP resin.

In this paper, the curing of a UP resin with methyl ethyl ketone peroxide (MEKP) as the initiator and cobalt octoate as the promoter, is studied by DSC at different heating rates β. A fixed initiator/promoter ratio was used. The DSC curves show an asymmetrical peak, which could be due to two different reactions taking place in the UP resins. The kinetic parameters have been obtained considering first, a single reactive process and second, two different reactive processes. For each DSC peak, a reaction rate given by $d\alpha_i/dt = k_i f(\alpha_i)$, with $i = 1{,}2$, has been assumed. If y represents the fraction of heat released during the first reaction, the relationship between the overall rate $d\alpha/dt$, determined experimentally in the curing by DSC calorimetry, and each particular rate of reaction, is:

$$\frac{d\alpha}{dt} = y\frac{d\alpha_1}{dt} + (1-y)\frac{d\alpha_2}{dt}. \tag{3}$$

2. Experimental

2.1. Materials and calorimetric instrumentation

A commercially available, general purpose UP resin, with the commercial name Estratil A-228, was used in this study. The base of the polyester consists of phthalic anhydride, maleic anhydride and propylene glycol, with a mole ratio of 3:2:5 obtained by ^{1}H NMR. The NMR peak for maleic anhydride was very small, because maleate groups isomerize extensively to fumarate groups during the synthesis of UP resins. The average weight of the unsaturated polyester was 1696 g/mol, and the equivalent molecular weight per mole C=C was 465 g/mol. The resin contains an average of 3.64 vinylene groups per polyester molecule. It was supplied with 35 wt.% of styrene as a cross-linking agent. The resin system has, approximately, a 2:1 styrene:polyester C=C molar ratio.

In curing the resin, a catalytic system was used: a 50% solution of MEKP in dibutyl phthalate was used as the initiator, with a 6% cobalt octoate (CoO) solution in phthalate as the promoter. The resin contains 70 ppm of hydroquinone as an inhibitor, to prevent premature polymerization during shipping and handling. This is a small amount in comparison with that of the initiator. Therefore, it is normally accepted that the inhibitor is totally consumed during the induction period and does not affect the reaction kinetics after that period. This assumption is commonly used to relate the consumption of initiator, the amount of effective inhibitor (inhibitor and oxygen) present, the decomposition constant of the initiator, and the induction time. Batch and Macosko [15] have proved that during isothermal DSC runs with resins and oxygen-active inhibitors such as hydroquinone, the induction time depends on the sample size, but the reaction kinetics, after inhibition, were unaffected by the amount of oxygen initially in the sample pan. Hence, even though inhibition is greatly affected by oxygen, the subsequent curing kinetics show no significant effect from the sample size [15]. It has also been verified [16] that during non-isothermal DSC runs at different heating rates, the induction period is unaffected by the sample size. The different behaviour of isothermal and non-isothermal experiments could be explained by the existence of a different rate between the initiation step and oxygen diffusion, since the length of inhibition [15] is determined by: (1) the initial oxygen concentration; (2) the rate of oxygen diffusion; and (3) the rate of radical initiation. If initiation is faster than diffusion, then the oxygen concentration in the resin will be low, and hence, inhibition time will be short.

The calorimetric measurements were carried out in a METTLER DSC equipped with a control and programming unit (microprocessor TC10 and calorimetric cell DSC20 arranged to permit temperature scans from − 10°C to 600°C). All DSC measurements were carried out in hermetic aluminium pans. A standard sample was prepared by mixing 10 g of UP resin with a fixed proportion of initiator and promoter (100:1:0.1) for approximately 1 min. The required amount of sample (20 mg) was weighed into a previously weighed sample pan, sealed, and placed in the DSC for each measurement. The pan can be filled with up to 40 mg. After each run, the weight of the sample was determined again to check any weight loss due to the evaporation of the styrene monomer. No significant weight loss was observed. The dynamic scans were performed from − 10°C to 200°C using a nitrogen atmosphere and different heating rates: 0.2, 2, 5, 10, 15, 20, 30 and 50°C/min. The DSC runs have been made up to a temperature value of 200°C to avoide the thermal decomposition of the cured resin. By means of thermogravimetric analysis (TG) of the A-228 resin used in this study, it has been proved that below the temperature of 250°C, the material is not degraded.

2.2. Experimental results

Fig. 1(a) represents the heat generated versus the cure temperature T_c, with the heating rate β as the parameter. The reaction rate versus at T_c a different heating rate is plotted in Fig. 1(b). It can be seen in Fig. 1(a) and (b) that: (1) the temperature at which the reaction begins increases with β; (2) the exothermic peak temperature increases β; (3) the temperature at which the completion of the cure reaction occurs increases with β; (4) the size of an exothermic peak increases with β; and (5) the shapes of the DSC curves (heat flow versus temperature) are non-symmetrical (see Fig. 1(b) and Fig. 2).

Rodriguez [17] studied a UP resin initiated with MEKP/CoO. He also found non-symmetrical DSC curves that were attributed to two exothermic peaks.

In Table 1, the exothermic DSC peak temperature T_p, the heat of reaction ΔH_R, and the degree of conversion, $\alpha = \alpha_p$, achieved when the temperature is equal to the exothermic peak temperature, is summarized. The heat of reaction ΔH_R was obtained as the next area:

$$\int_0^{t_c} \left(\frac{dH}{dt}\right)_T dt, \tag{4}$$

where t_c is the curing time (i.e. the time necessary for the DSC trace to return to the baseline), and $(dH/dt)_T$ is the calorimetric signal during the experimental DSC run.

As can be seen in Table 1, the amount of heat generated by a curing reaction is independent of β in the range 5–30°C/min. Even though the size of exothermic peak and the reaction rate increase with β, the time of curing, t_c, decreases with β. Thus, when a low heating rate is used, the calorimetric signal, $(dH/dt)_T$, is small, but the curing time is great. The opposite occurs at a high heating rate, where the reaction heat ΔH_R is released in a short period of time. Therefore, the area of the calorimetric signal, i.e. the integral:

$$\int_0^{t} \left(\frac{dH}{dt}\right)_T dt,$$

can be expected to be constant. Other investigators [18]–[22] have found a similar result. These results suggest the existence of an optimum range for the heating rate. For values lower than 5°C/min, some of the initial reaction and the final reaction can be unrecorded, because of a lack of calorimeter sensitivity. For values higher than 30°C/min, endothermal reaction (i.e. a possible evaporation of styrene: the pressure which can be reached in the closed DSC pan is approximately 2 bar. At this pressure, the boiling point of styrene is approximately 140°C) of the material can occur simultaneously to curing, and it may decrease the exothermicity of the reaction. An average value of 345 J/g was assigned to the heat of polymerization of the UP resin. Other investigators [23,24] have reported a range of heat of polymerization from 292.6 J/g to 426 J/g for UP resins. This range may be due to the different types of UP resins and free-radical initiator systems employed in each study

Table 1
Total heat of reaction, ΔH_R, peak temperature, T_p, and degree of conversion of the peak, α_p, at different heating rates β

β (°C/min)	ΔH_R (J/g)	T_p (°C)	α_p
0.2	306.0	33.3	0.42
2	324.9	67.2	0.42
5	344.6	89.8	0.62
10	346.9	112.1	0.71
15	351.7	125.3	0.71
20	342.6	132.7	0.71
30	352.1	146.0	0.70
50	336.2	159.4	0.64

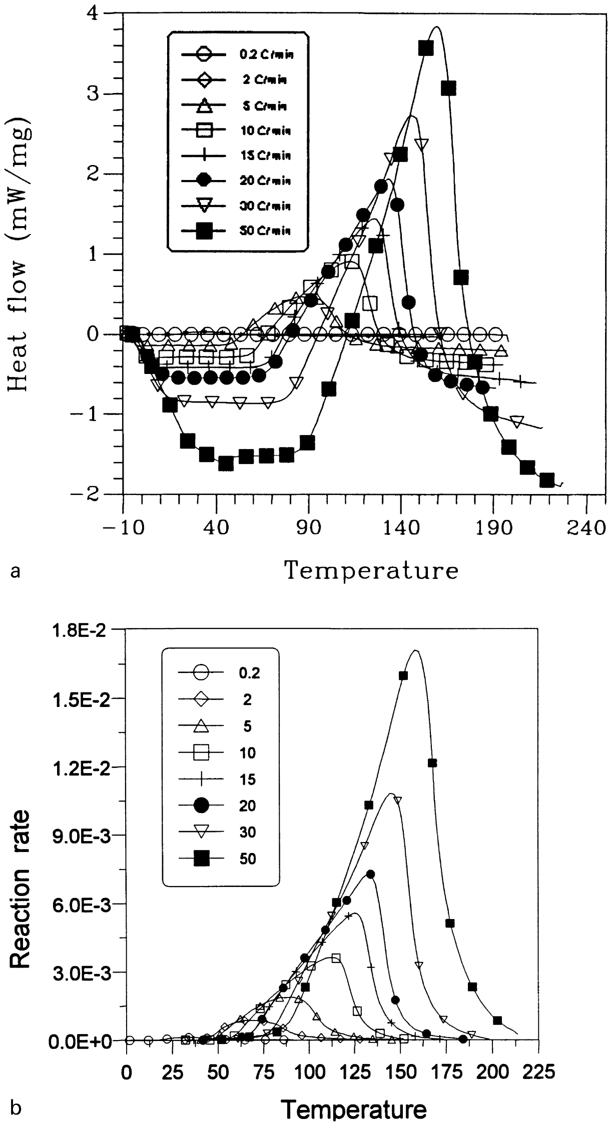

Fig. 1. (a) DSC heat flow dH/dt versus temperature (°C) for dynamic scans at different heating rates; (b) reaction rate versus temperature for dynamic scans at different heating rates.

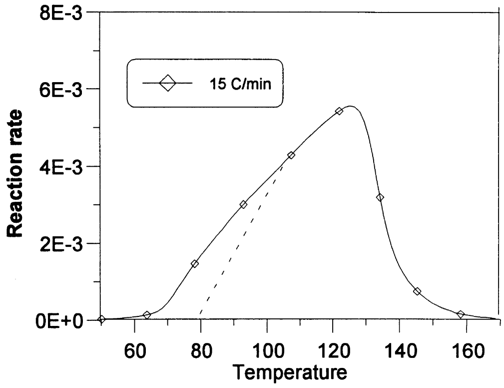

Fig. 2. Reaction rate dα/dt versus temperature (°C) for a dynamic scan (β = 15°C/min).

[2]. Basically, the reaction heat ΔH_R is due to a cross-linking reaction between the polyester double bonds and the styrene double bonds. However, the organic peroxide decomposition is a highly exothermal reaction (for instance, the heat released in the decomposition [25] of pure benzoyl peroxide measured by DSC is 400 J/g), and different amounts of initiator can give different values for ΔH_R. Nevertheless, the heat involved in the decomposition of the initiator is comparatively negligible given the small amount of peroxide present in the formulation.

From the dependence between β and T_p, it is possible to obtain the activation energy, E, using the Ozawa method. In the Ozawa calculation procedure [26], the following equation is derived:

$$\ln\beta = \text{constant} - 1.052\frac{E}{RT_p}. \tag{5}$$

This expression shows a linear dependence of the reciprocal absolute peak temperature on the logarithm of the heating rate. The activation energy E (kJ/mol) is calculated from the slope of the straight line obtained (Ozawa plot), either graphically or by linear regression. A good fit was observed with a regression coefficient of $r = 0.989$. A value of $E = 45.8$ kJ/mol was obtained.

3. Theoretical part

3.1. Kinetic model

It has been assumed that the curing reaction of a UP resin with a mixture of initiator and promoter, involves two independent reactions. Therefore, the following assumptions have been made:

(a) The resin system is formed by a set of two independent cross-linking reactions. Each reaction obeys a rate law of the form:

$$\frac{d\alpha_i}{dt} = k_i(T)f(\alpha_i) \quad i = 1, 2, \tag{6}$$

where the dependence upon α_i from the dependence upon T has been separated. The rate constant $k_i(T)$ for each reaction differs significantly, so that the position of exothermic peaks for each individual reaction is not affected and can be clearly distinguished. The dependence upon the temperature of $k_i(T)$ follows an Arrhenius-type equation:

$$k_i(T) = A_i \exp(-E_i/RT), \tag{7}$$

where A_i is the frequency factor and E_i is the activation energy.

(b) Two different expressions for $f(\alpha_i)$ have been used in this study:

nth – order reaction $(1-\alpha_i)^n$,

autocatalysed $\alpha_i^m(1-\alpha_i)^n$.

(c) The relationship between the total heat ΔH_R and the individual heats of reaction ($\Delta H_{R,i}$) is:

$$\Delta H_R = \Delta H_{R,1} + \Delta H_{R,2}, \tag{8}$$

where $\Delta H_{R,1}$ and $\Delta H_{R,2}$ are the total heat released during the first and the second reactions, respectively. Therefore, the overall degree of reaction, α, for this system, can be related to the individual degree of reaction α_i, by means of:

$$\alpha = y\alpha_1 + (1-y)\alpha_2, \tag{9}$$

where y is the fraction that corresponds to the first process of the reaction. It can be obtained as the relationship between the area under the first peak (e.g. the heat of the first reaction $\Delta H_{R,1}$) and the area under the DSC thermogram (e.g. the total heat of reaction ΔH_R):

$$y = \frac{\Delta H_{R,1}}{\Delta H_R} = 1 - \frac{\Delta H_{R,2}}{\Delta H_R}. \tag{10}$$

(d) The heat released per unit mass of resin is given by:

$$\frac{dH}{dt} = \Delta H_{R,1}\frac{d\alpha_1}{dt} + \Delta H_{R,2}\frac{d\alpha_2}{dt}, \tag{11}$$

where 1 and 2 refer to the first and the second cross-linking reactions, respectively. dH/dt is the ordinate of the DSC curve obtained experimentally. The experimental values of dH/dt cannot be fitted directly to the above expression, as the fractional conversion α_i for each individual peak, and the fraction y, are unknown. This expression can be transformed and written as:

$$\frac{d\alpha}{dt} = y\frac{d\alpha_1}{dt} + (1-y)\frac{d\alpha_2}{dt} = yk_1(T)f(\alpha_1) + (1-y)k_2(T)f(\alpha_2). \tag{12}$$

This will be used in fitting the experimental data. In the calculation procedure, the corresponding kinetic parameters are computed by applying the downhill simplex algorithm [27,28] (which generates a set of kinetic parameters) and, the Runge–Kutta numerical method [29,30] to solve differential equations, and thus, to obtain the degree of conversion for each peak (α_i) as a function of temperature. The computing algorithm gives the set of kinetic parameters that minimizes the χ^2-merit function (also called the chi-squared function) defined as:

$$\chi^2(\boldsymbol{a}) = \sum_{i=1}^{N}[z_{\exp,i} - z_{\text{calc}}(T_i, \boldsymbol{a})]^2, \tag{13}$$

where N is the number of experimental values, z represents the reaction rate measured, $d\alpha/dt$ (exp) or calculated (calc) from the kinetic parameters **a**, and T_i denotes the temperature. A smaller value for the merit function denotes a better agreement between the experimental data points and the theoretical model. This iterative calculation algorithm has been explained in previously (see Ref. [31]).

4. Results

The kinetic analysis of thermosetting cures involves a search for the kinetic parameters (A, E, n, m) of the process, according to a mechanistic model that fits the experimental

Table 2
Kinetic parameters, coefficient of correlation, *r*, and chi-squared function for the different fits of experimental data realized considering one process and using an *n*th-order function $f(\alpha)$, at different heating rates β

β (°C/min)	ln*A*	*E* (kJ/mol)	*n*	$\chi^2(a)$	*r*
0.2	23.88	81.8	1.44	1.21×10^{-8}	0.872
2	17.27	67.0	1.13	5.25×10^{-7}	0.898
5	17.07	67.0	1.14	6.86×10^{-7}	0.949
10	14.51	61.0	0.86	2.77×10^{-6}	0.945
15	14.79	61.7	0.78	7.77×10^{-6}	0.942
20	14.23	61.2	1.00	1.24×10^{-5}	0.901
30	14.82	64.0	0.76	2.23×10^{-5}	0.940
50	15.40	66.0	0.97	7.21×10^{-5}	0.920

data. For each non-isothermal DSC curing, the required properties (degree of conversion α and reaction rate dα/d*t* as time or temperature functions) were evaluated by using Eqs. (1) and (2). It was assumed that the dynamic heat obtained as the area of the DSC thermogram, represents the total reaction heat of polymerization. Therefore, a 100% conversion was reached in all curing reactions carried out at different heating rates. In order to compare the results obtained and to point out differences between them, two types of adjustments were carried out. First, the experimental data were fitted considering a single reaction. Afterwards, another set of kinetic parameters corresponding to two reactions was also obtained.

4.1. One single process

Table 2 gives the kinetic parameters obtained for each heating rate, considering one single process and using an *n*th-order function *f*(α). The chi-squared function $\chi^2(a)$ and the coefficient of correlation *r*, are also given. In general, the kinetic parameters are not constant and show a dependence upon the heating rate. In the range of heating rate of 10–30°C/min, the energy of activation *E* seems to be constant with an average value of 61.9 kJ/mol. For the logarithm of frequency factor (ln*A*) and the reaction order *n*, the average values of 14.58 and 0.85 were obtained, respectively. In this range of heating rates, the fitting of experimental data is better (*r* values closer to unity) than those obtained at other heating rates (*r* values smaller).

Fig. 3 gives a comparison of the computed dα/d*t* versus the cure temperature curves, considering one single process and using an *n*th-order function *f*(α), with experimental results at different heating rates. As is apparent, the calculated curves do not fit well with the experimental data at the beginning and the termination of the cure process. The peak temperature T_p associated with the calculated curves is shifted when compared with the T_p of the experimental curves. This effects are more pronounced at low heating rates.

The kinetic parameters obtained at each heating rate, when considering one single process and using an autocatalysed function *f*(α), are given in Table 3. The considerations made to the *n*th-order function results apply here also. In the range of heating rate of 5–20°C/min, the energy of activation is practically constant, with an average value of 52.9 kJ/mol. The reaction orders *m* and *n*, and the sum $n + m$, are also constant, with average values of 0.15, 0.73 and 0.88, respectively. In this range, the fits of experimental data are better than those for other heating rates. In comparison with the *n*th-order function, the fits are better at low heating rates, but they are comparable in the range of $\beta = 5$–50°C/min. Therefore, in this range, it is not possible to distinguish between the results obtained with both models of *f*(α). In Fig. 4, the curves of the computed dα/d*t* versus the cure temperature curves, and the experimental results at different heating rates, are given. It can be seen that the fit of experimental data at low heating rates and using the autocatalysed function *f*(α), is better than the one that considers the *n*th-order function *f*(α).

Table 3
Kinetic parameters, coefficient of correlation, *r*, and chi-squared function for the different fits of experimental data realized considering one process and using an autocatalysed function $f(\alpha)$, at different heating rates β

β (°C/min)	ln*A*	*E* (kJ/mol)	*m*	*n*	$\chi^2(a)$	*r*
0.2	14.45	55.7	0.57	1.99	3.87×10^{-9}	0.932
2	13.97	55.6	0.46	1.68	2.14×10^{-7}	0.937
5	13.42	53.5	0.24	1.17	6.26×10^{-7}	0.952
10	12.17	52.9	0.12	0.83	2.77×10^{-6}	0.945
15	11.82	50.1	0.14	0.75	7.84×10^{-6}	0.941
20	10.69	55.1	0.11	0.63	1.10×10^{-5}	0.902
30	12.28	60.8	0.13	0.73	2.27×10^{-5}	0.939
50	13.25	58.5	0.15	0.90	7.58×10^{-5}	0.919

4.2. Two processes

Table 4 summarizes the set of kinetic parameters obtained for each heating rate, considering two processes and using an *n*th-order function of reaction *f*(α) for each process. The coefficients of correlation, *r*, obtained have similar values as those obtained with one single process of reaction. Nevertheless, there is an improvement at low heating rates. The values of activation energy of the second peak seem to be constant, with an average value of 88.4 kJ/mol. For the first peak, the activation energy depends on the heating rate, with an average value of 51.5 kJ/mol. The average value of the activation energy corresponding to one single process ($E = 61.9$ kJ/mol) is in the range of these energies of activation (50–90 kJ/mol). The fraction *y* decreases as the heating rate increases.

In Fig. 5, the curves corresponding to the computed dα/dt versus the cure temperature, using two kinetic peaks and *n*th-order functions *f*(α_1) and *f*(α_2), and the experimental results at different heating rates, are given. The two simulated peaks are also drawn in Fig. 5 for each heating rate. As can be seen, there are still some discrepancies between the fitting curves and the experimental data. In addition, the beginning of the first and the second curves are very close. This would mean that the two reactive processes are simultaneous, and not different processes, as has been assumed.

In Table 5, the kinetic parameters obtained for each heating rate by considering two independent kinetic processes of

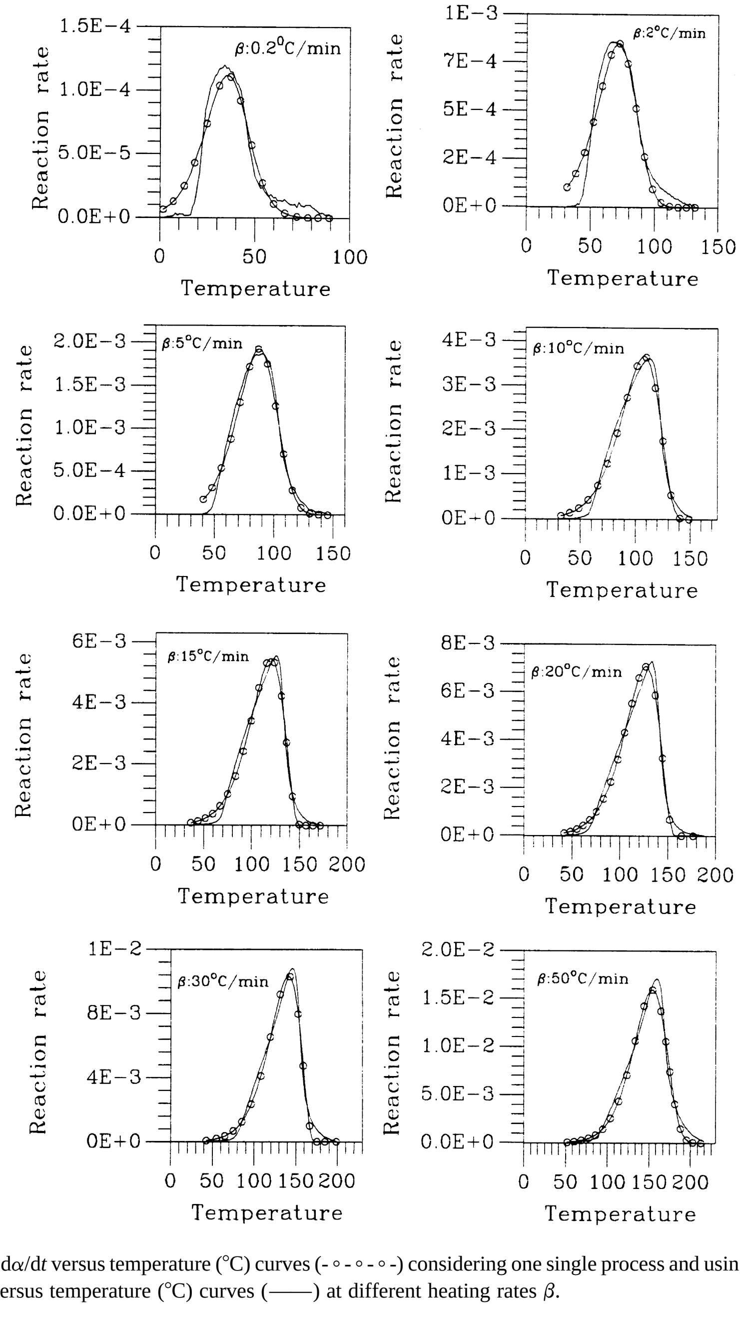

Fig. 3. The calculated reaction rate dα/dt versus temperature (°C) curves (- ◦ - ◦ - ◦ -) considering one single process and using an *n*th-order function $f(\alpha)$, and the experimental reaction rate dα/dt versus temperature (°C) curves (——) at different heating rates β.

Table 4
Kinetic parameters for each individual reaction, fraction *y*, coefficient of correlation, *r*, and chi-squared function for the different fits of experimental data realized considering two processes and using an *n*th-order function *f*(α), at different heating rates β

β (°C/min)	A_1 (s^{-1})	E_1 (kJ/mol)	n_1	y	A_2 (s^{-1})	E_2 (kJ/mol)	n_2	χ^2(a)	r
0.2	7.06×10^6	62.0	0.63	0.825	1.33×10^8	73.4	1.12	1.42×10^{-8}	0.852
2	5.80×10^5	56.7	0.95	0.735	8.02×10^{10}	87.6	1.05	5.10×10^{-7}	0.896
5	1.83×10^5	53.4	0.90	0.684	1.03×10^{11}	90.3	1.04	9.47×10^{-7}	0.938
10	6.75×10^3	44.5	0.43	0.597	5.14×10^{10}	90.8	1.75	3.03×10^{-6}	0.939
15	1.71×10^4	47.7	0.31	0.564	7.60×10^9	86.4	1.65	7.53×10^{-6}	0.941
20	1.63×10^4	47.6	0.29	0.498	4.94×10^9	85.8	1.66	1.23×10^{-5}	0.940
30	1.95×10^4	48.6	0.26	0.422	5.56×10^9	88.5	1.57	1.86×10^{-5}	0.943
50	1.99×10^4	48.8	0.23	0.303	5.80×10^9	89.9	1.66	6.03×10^{-5}	0.941

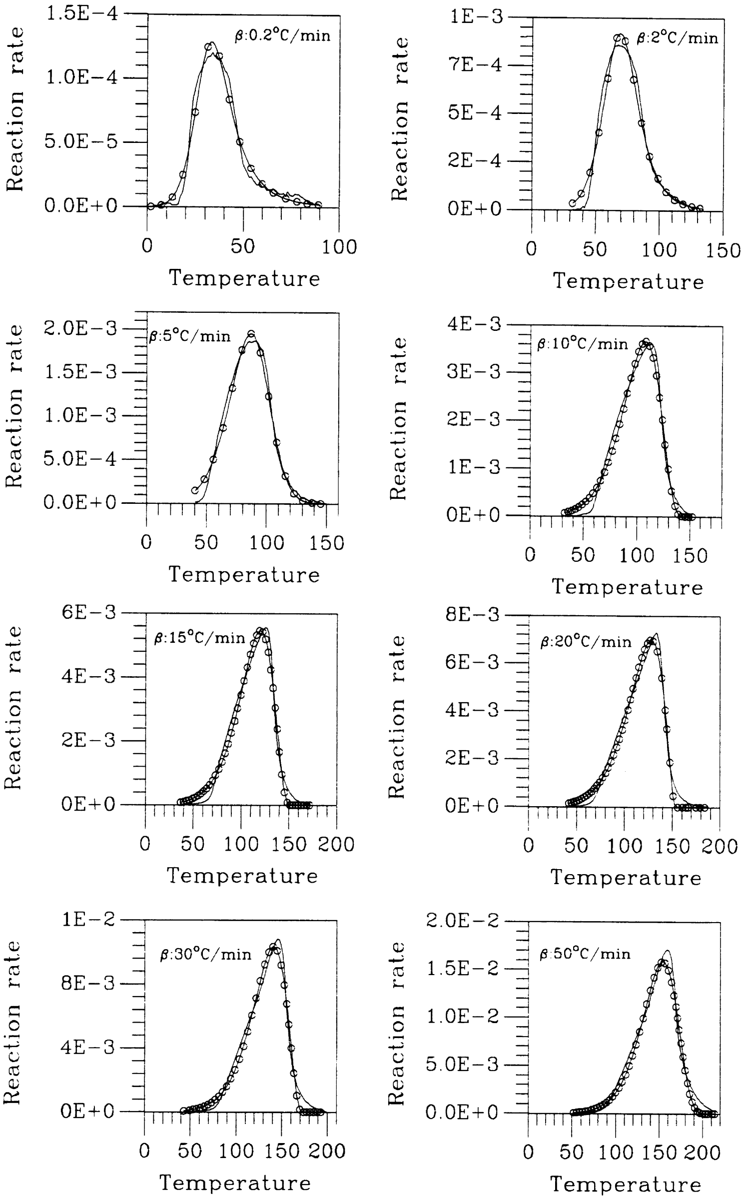

Fig. 4. The calculated reaction rate dα/dt versus temperature (°C) curves (- ∘ - ∘ - ∘) considering one single process and using an autocatalysed function $f(\alpha)$, and the reaction rate experimental dα/dt versus temperature (°C) curves (——) at different heating rates β.

Table 5
Kinetic parameters for each individual reaction, fraction y, coefficient of correlation, r, and chi-squared function for the different fits of experimental data realized considering two processes and using an autocatalysed function $f(\alpha)$, at different heating rates β

β (°C/min)	A_1 (s^{-1})	E_1 (kJ/mol)	m_1	n_1	y	A_2 (s^{-1})	E_2 (kJ/mol)	m_2	n_2	$\chi^2(a)$	r
0.2	3.89×10^4	46.1	0.60	1.64	0.962	7.23×10^9	86.8	0.57	1.24	3.48×10^{-9}	0.933
2	3.70×10^4	43.7	0.70	2.01	0.732	9.71×10^9	81.5	0.63	1.77	5.26×10^{-8}	0.969
5	2.74×10^4	43.6	0.55	1.57	0.696	2.56×10^{10}	87.0	0.45	1.30	1.74×10^{-7}	0.974
10	2.94×10^4	43.7	0.54	1.63	0.597	2.59×10^{10}	89.8	0.36	1.02	5.78×10^{-7}	0.974
15	3.08×10^4	43.4	0.58	1.71	0.508	2.52×10^{10}	91.3	0.31	0.98	1.62×10^{-6}	0.973
20	3.27×10^4	43.3	0.55	1.76	0.436	1.76×10^{10}	91.5	0.16	0.86	2.18×10^{-6}	0.975
30	2.56×10^4	42.4	0.61	2.14	0.402	7.16×10^9	90.0	0.19	0.89	7.13×10^{-6}	0.966
50	1.19×10^4	40.9	0.54	2.05	0.305	2.80×10^8	79.6	0.24	1.03	4.61×10^{-5}	0.948

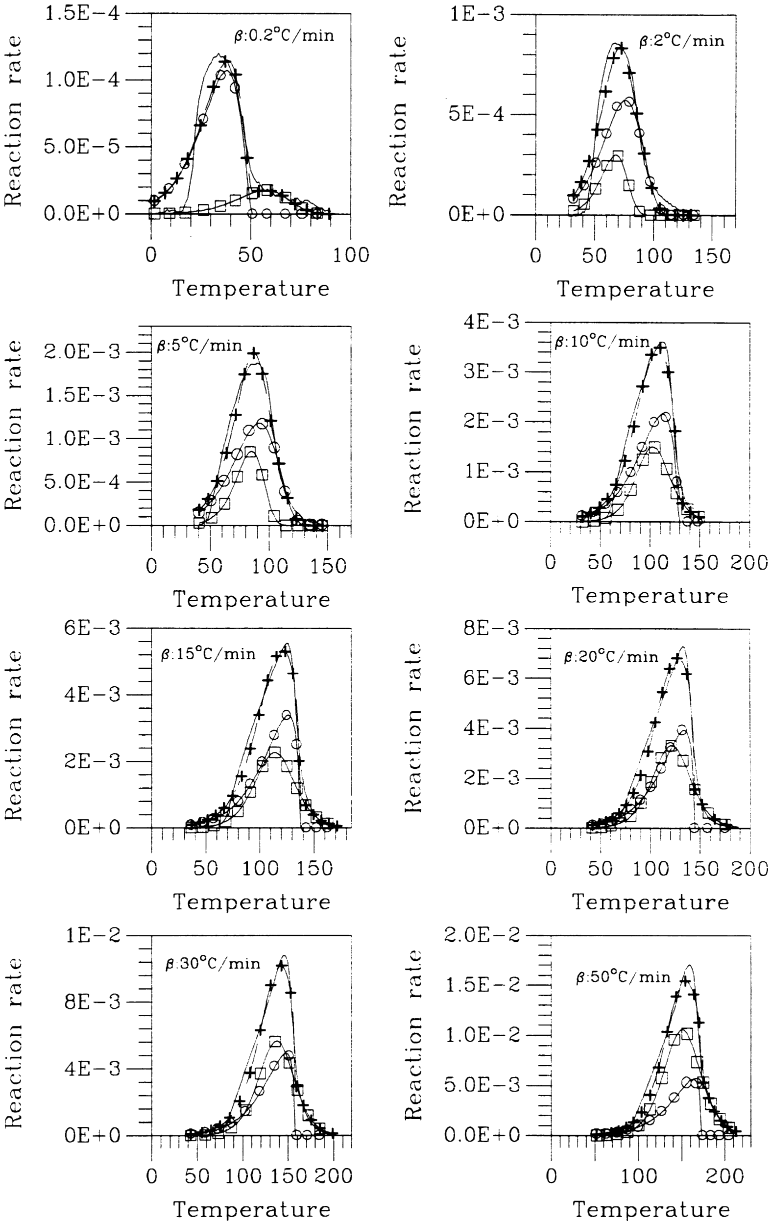

Fig. 5. The calculated reaction rate dα/dt versus temperature (°C) curves (+ − + − +) considering two processes and using an nth-order function $f(\alpha)$, and the experimental reaction rate dα/dt versus temperature (°C) curves (——) at different heating rates β. The first (○○○) and the second (□□□) simulated peaks are also drawn.

reaction and using an autocatalysed function, $f(\alpha)$, for each process, are given. The correlation coefficients for each heating rate are greater than the *r* values for any other fitting at the same heating rates. In these fits, the fraction *y* also decreases as the heating rate increases. In this case, there are two different reactive processes, as is shown in Fig. 6. For each heating rate, the first peak always occurs before the second peak. At low heating rates, the first peak is greater than the second peak. On the contrary, at high heating rates, the first peak is smaller than the second peak. The values of activation energy for each peak are practically constant with β. For the first peak, an average value of 43.4 kJ/mol was obtained, and for the second peak, a value of 87.2 kJ/mol was found. These values of activation energy are in accordance with the values tabulated in the literature, corresponding to a free-radical polymerization initiated by the redox decomposition of the initiator at low temperatures, and a free-radical polymerization initiated by the thermal decomposition of the initiator at high temperatures, respectively.

If we assume that these two reactions are two polymerization processes with two initiation mechanisms: redox decomposition of peroxide at low temperatures and thermal decomposition of peroxide at high temperatures, the results obtained in this work can be explained. At low heating rates, the sample temperature increases slowly and a large period

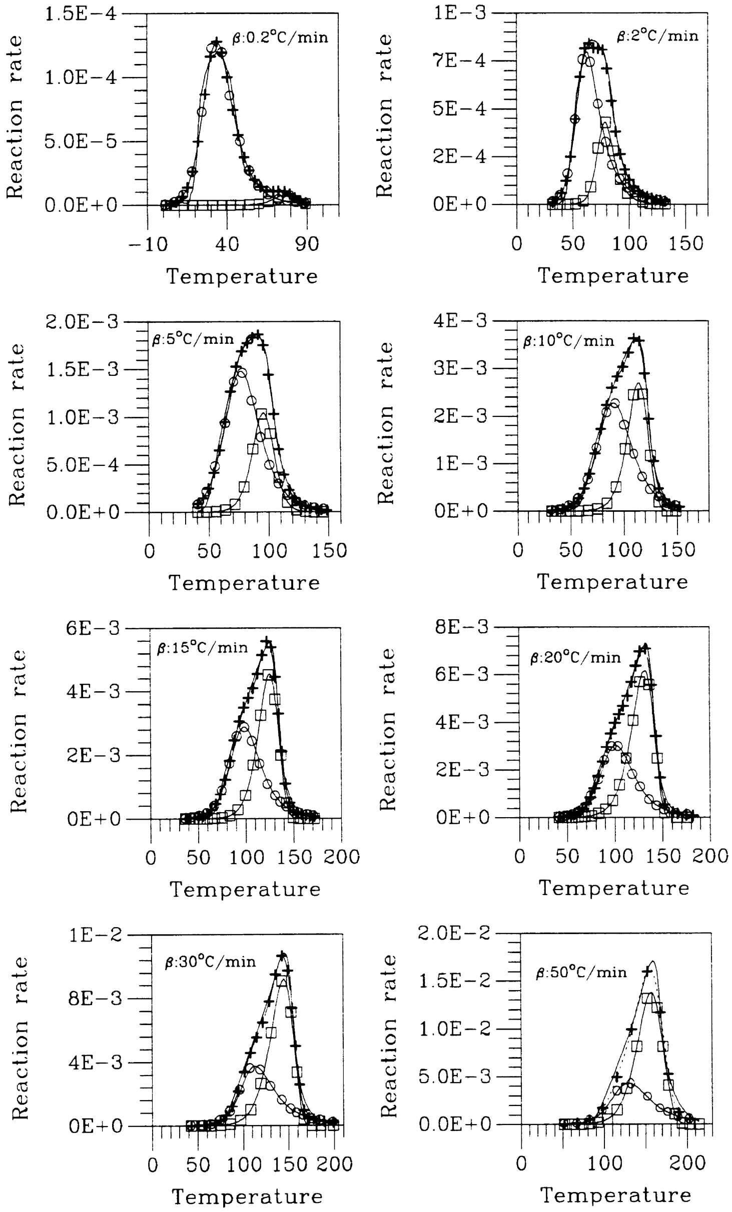

Fig. 6. The calculated reaction rate dα/dt versus temperature (°C) curves (+ − + − +) considering two processes and using an autocatalysed function $f(\alpha)$, and the experimental reaction rate dα/dt versus temperature (°C) curves (——) at different heating rates β. The first (○○○) and the second (□□□) simulated peaks are also drawn.

is required to reach high values of temperature, which induces thermal decomposition of the peroxide initiator. Therefore, the redox decomposition of the peroxide initiator is the prevailing phenomenon when the heating rate is low. On the contrary, the temperature of the sample increases strongly when high heating rates are used. In a short period, the temperature reaches a high value and the thermal decomposition of the peroxide initiator begins rapidly. Thus, at high heating rates, the thermal decomposition competes with and dominates the redox decomposition of the peroxide initiator.

5. Discussion

DSC is a relatively simple technique that provides cure kinetic information and allows the identification of one or more reactions. However, the disadvantage of this technique in the cure analysis, is that the heat of reaction does not necessarily reflect the cross-linking formation. Each chemical reaction produces heat, regardless of whether a cross-link is formed or not. In these cases, other techniques are required.

The curing of a UP resin is a free-radical polymerization in which the resin is transformed from the liquid state into a rigid cross-linked molecular structure. To induce the production of free radicals in the system, either heat or a catalytic system is required [25,32,33]. It is customary practice to associate an overall activation energy to a steady-state, free-radical polymerization, such as the curing of UP resins, by combining three separate Arrhenius-type equations for each occurring process [initiation (d), propagation (p) and termination (t)] [34]. In this case, the temperature dependence of the rate constant is generally given by an Arrhenius constant relationship:

$$k(T) = A_0 \exp\left(-\frac{E}{\mathrm{R}T}\right) = \frac{A_\mathrm{d}^{1/2} A_\mathrm{p}}{A_\mathrm{t}^{1/2}} \exp\left(\frac{(E_\mathrm{d} + 2E_\mathrm{p} - E_\mathrm{t})/2}{\mathrm{R}T}\right), \tag{14}$$

where E is the activation energy, R the gas constant, and A_0 an Arrhenius constant. When the process of reaction is only initiated by thermal decomposition of the initiator, the overall activation energy for most free radical polymerizations is approximately 80–90 kJ/mol. (The values of E_p, E_t and E_d for free-radical polymerization of styrene with peroxybenzoate initiator, are 26, 8.0 and 134 kJ/mol, respectively [34].) Thus, the activation energy for the polymerization of styrene is $E = E_\mathrm{d}/2 + E_\mathrm{p} - E_\mathrm{t}/2 = 89$ kJ/mol. These results suggest that the second reaction considered here could be produced by a mechanism of thermal initiation. Recently, Martín et al. [31] studied dynamically, by DSC, the curing of this resin, with MEKP as the initiator at different heating rates. The polymerization was only initiated by thermal decomposition of MEKP. The positions of DSC peaks appearing in there work coincide with the position of the second peak studied in the present paper, and the values of activation energies are in accordance with the values for the second peak found here.

When there is only a redox initiation, the value of the overall activation energy is approximately one-half of the value for non-redox initiations. That is approximately 40–60 kJ/mol [34]. Among the three steps involved in the polymerization, the initiation activation energy is the only one that changes. The value of 40 kJ/mol for the activation energy, might seen unrealistic of the UP resin curing. Normally, values of 60 kJ/mol, such as those found in this paper, when only one process is considered, are more realistic. However, when the polymerization is promoted by free radicals as the UP resin curing, Odian [34] summarizes values in the range of 40–60 kJ/mol for redox initiation. Grentzer et al. [35] studied a novolac-modified vinyl ester initiated with benzoyl peroxide (BP), with *n*-dimethylaniline (DMA) as the promoter, at different heating rates (40, 30, 20, 10, 7.5, 5, 3.8 and 2.5°C/min). They found two different exothermic peaks, which shift to lower temperatures as the experimental heating rate is decreased. For the first peak, which they attributed to the chemical decomposition reaction of BP by the DMA promoter, they found an activation energy of 46.1 kJ/mol. The second peak had an activation energy of 123 kJ/mol, which agrees very well with the activation energy reported for the thermal decomposition of BP.

In several works, two distinctly different reactions have been identified by DSC analysis, for UP resins catalysed with an initiator and a promoter. The thermograms show that the exothermic peaks vary in size and position as the concentration of MEKP and cobalt octoate are altered. In the literature, there is controversy about the origin of these exothermic peaks. Avella et al. [36] suggested that the first peak was due to the copolymerization of the styrene with the polyester unsaturation, while the second peak was caused by styrene homopolymerization. That interpretation is arguable, since the copolymerization is the prevailing reaction [37–39], because styrene monomer in the UP resins is always present at a level stoichiometrically in excess to the polyester [39]. Moreover, the homopolymerization of polyester takes place at temperatures higher than 150°C, far from the range of curing temperatures for the greatest number of DSC runs. For example, in the case of UP resin, polymerization in the absence of an initiator occurs in a temperature range of 180°C–210°C. The same occurs with the styrene homopolymerization. (Pure styrene, without any initiator, polymerizes in a range of temperatures between 140°C and 310°C.)

Salla et al. [40] also studied the curing kinetics for UP resins by varying the cobalt octoate concentration. They attributed the first peak to polymerization initiated by a redox decomposition of MEKP, and the second to polymerization initiated by the thermal decomposition of MEKP at high temperatures. Other investigators [17,35,41,42] have made a similar interpretation in studies on vinyl ester resins and polyester resins. Recently, Cook et al. [43] attributed these peaks to the individual influence of temperature on each of the fundamental reaction steps in the free-radical polymerization. Jacobs and Jones [44] studied by DMTA, a UP resin with MEKP and different concentrations of cobalt octoate. They found the existence of a heterogeneous structure, which consists of highly cross-linked domains surrounded by less highly cross-linked areas, and arises as a result of the statistics of the free-radical cure of the resin. Given this controversy, other spectroscopic and structural analysis should be made to know what is the correct interpretation about the origin of the two reactive processes found here.

6. Conclusions

The curing of a UP resin initiated with MEKP peroxide and cobalt octoate as the promoter, has been studied by DSC. Non-isothermal scanning was performed at different heating rates. The shapes of experimental heat-flow DSC curves are non-symmetrical. This indicates that two independent reactions could be taking place. The kinetic parameters A, E, n and m, and the fraction y, were determined by using an iterative computation algorithm. From the study of calculated data and their comparison with experimental results, it can be concluded that:

1. The fits of experimental data are poor (e.g. coefficient of correlation r is smaller) when one single process of the reaction [either nth-order or autocatalysed function $f(\alpha)$] is considered in monitoring the curing. Moreover, there are not significant differences between the results obtained by using both models. The beginning, shape and size of experimental DSC curves depend on the heating rate β. The values of activation energy corresponding to one single reaction, also depend on β. Their average value is greater than the value obtained from kinetic methods based on roughly approximate formulae, such as the Ozawa method, and it is in the range determined by the energies of activation corresponding to each independent cure reaction.
2. The fits of experimental data are better when two independent reactions are considered. With regard to $f(\alpha)$, it is possible to distinguish, in this case, between the results obtained with the nth-order function and with the autocatalysed function. When the nth-order function is used in the kinetic model, the two reactions seem to be simultaneous. Instead, when the autocatalysed function $f(\alpha)$ is used, the second peak occurs after the first peak. Moreover, the experimental data are of a better fit than with any other type of fit considered in this work. These two reactions are in competition, and one of them becomes the prevailing phenomenon, depending on the established heating rate. Precisely the fraction y of the first peak decreases as the heating rate increases. The values of energies of activation obtained with this model, are in accordance with the values tabulated for free radical polymerizations initiated by redox or by thermal peroxide decomposition, respectively.
3. The presence of more than one peak indicates the complexity of the curing and reflects the importance that the catalytic system has, not only on the rate of cure, but also in the final reaction extent. In our case, two reactions have been assumed in the dynamic curing. Several controversial interpretations can be found in the literature about the origin of these reactions. Other studies that use spectroscopic and structural analysis techniques should be made, to find the cause of these reactions. Nevertheless, the mathematical, kinetic model used in this work, is independent of these interpretations, and can be used to fit the experimental data of other thermosetting systems, which present more than one DSC peak.

References

[1] Worthy W. Chem Engng News 1987;16:7.
[2] Prime RB. In: Turi E, editor. Thermal characterization of polymeric materials, chap. 5. New York: Academic Press, 1981.
[3] Duswalt AA. Thermochim Acta 1974;8:57.
[4] Brown ME. Introduction to thermal analysis. London: Chapman and Hall, 1988.
[5] Widman G. In: Application mettler no. 802, 1986.
[6] Riesen R, Widman G. Thermal analysis, term, methods, applications. Heidelberg: Hütching Verlag, 1987.
[7] Stevenson JF. Polym Engng Sci 1986;26:746.
[8] Chern CS, Sundberg DC. ACS Polym Preprints 1985;26 (1):296.
[9] Horie K, Mita I, Kambe H. J Polym Sci 1969;7:2561.
[10] Han CD, Lee D. J Appl Polym Sci 1987;33:2859.
[11] Kamal MR, Sourour S. Polym Engng Sci 1973;13:59.
[12] Ryan ME, Dutta A. Polymer 1979;20:203.
[13] Pusatcioglue SY, Fricke AL, Hassler JC. J Appl Polym Sci 1979;24:937.
[14] Lem KW, Han CD. J Appl Polym Sci 1983;28:3155.
[15] Batch GL, Macosko CW. Thermochim Acta 1990;166:185.
[16] Martín JL, Salla JM, Ramis X, Cadenato A. J Therm Anal 1992;38:91.
[17] Rodriguez EL. Polym Engng Sci 1991;31:1022.
[18] King PW, Mitchell RH, Westwood AR. J Appl Polym Sci 1974;18:1117.
[19] Prime RB. Polym Engng Sci 1973;13:365.
[20] Fava RA. Polymer 1968;9:137.
[21] Sourour S, Kamal MR. Thermochim Acta 1976;14:41.
[22] Salla JM, Martín JL. Thermochim Acta 1988;126:339.
[23] Cuadrado TR, Borrado J, Williams RJ, Clara FM. J Appl Polym Sci 1983;28:485.
[24] Ng H, Mana-Zloczower I. Polym Engng Sci 1989;29:1097.
[25] Severini F, Gallo R. J Therm Anal 1985;30:841.
[26] Ozawa T. J Therm Anal 1970;2:301.
[27] Nelder JA, Meal R. Comput J 1965;7:308.
[28] Press WH, Tenkolsky SA, Vetterling WT, Flaunery BP. Numerical recipes in Fortran, 2nd ed., chap. 10. New York: Cambridge University Press, 1992.
[29] Jenson VG, Jeffreys GV. Mathematical methods in chemical engineering. London: Academic Press, 1977.
[30] Smith JM. Reaction kinetics for chemical engineers, 3rd ed. New York: McGraw-Hill, 1985.

[31] Martín JL, Cadenato A, Salla JM. Thermochim Acta 1997;306:115.

[32] Yang YS, Suspéne L. In: Proceedings of the 46th Annual Conference, Composites Institute. The Society of Plastics Industry. February 18–21, 1991, session 10-A.

[33] Selley J. In: Encyclopedia of polymer science and engineering, vol. 12. New York: Wiley, 1984:257–290.

[34] Odian G. Principles of polymerization, 3rd ed. New York: Wiley, 1991.

[35] Grentzer TH, Rust DA, Lo SK, Spencer CJ, Hackworth GW. In: Proceedings of the 46th Annual Conference, Composites Institute. The Society of Plastics Industry. February 18–21, 1991, session 1-B.

[36] Avella M, Martuscelli E, Mazzola M. J Therm Anal 1985;30:1359.

[37] Lewis FM, Walling C, Cummings W, Briggs ER, Mayo FR. J Am Chem Soc 1948;70:1519.

[38] Horie K, Mita I, Kambe H. J Polym Sci (A-1) 1969;7:2561.

[39] Yang YS, Lee LJ. Polym Pro Engng 1987;5:327.

[40] Salla JM, Ramis X, Martín JL, Cadenato A. Thermochim Acta 1988;134:261.

[41] Lem KL, Han CD. Polym Engng Sci 1984;24:175.

[42] Yang YS, Lee LJ. Polym Pro Engng 1987;5:327.

[43] Cook WD, Simon GP, Burchill PJ, Lau M, Fitch TJ. J Appl Polym Sci 1997;64:769.

[44] Jacobs PM, Jones FR. Polymer 1992;33 (7):1418.